

Modern Physics Letters B
© World Scientific Publishing Company

Competing Phases in Spin- $\frac{1}{2}$ J_1 - J_2 Chain with Easy-Plane Anisotropy

Masahiro Sato¹, Shunsuke Furukawa², Shigeki Onoda³ and Akira Furusaki³

¹*Department of Physics and Mathematics, Aoyama Gakuin University, Sagamihara, Kanagawa 252-5258, Japan*

²*Department of Physics, University of Toronto, Toronto, Ontario, Canada M5S 1A7*

³*Condensed Matter Theory Laboratory, RIKEN, Wako, Saitama 351-0198, Japan*

Received (Day Month Year)

Revised (Day Month Year)

We summarize our theoretical findings on the ground-state phase diagram of the spin- $\frac{1}{2}$ XXZ chain having competing nearest-neighbor (J_1) and antiferromagnetic next-nearest-neighbor (J_2) couplings. Our study is mainly concerned with the case of ferromagnetic J_1 , and the case of antiferromagnetic J_1 is briefly reviewed for comparison. The phase diagram contains a rich variety of phases in the plane of J_1/J_2 versus the XXZ anisotropy Δ : vector-chiral phases, Néel phases, several dimer phases, and Tomonaga-Luttinger liquid phases. We discuss the vector-chiral order that appears for a remarkably wide parameter space, successive Néel-dimer phase transitions, and an emergent nonlocal string order in a narrow region of ferromagnetic J_1 side.

Keywords: frustration, one-dimensional quantum magnets, infinite time evolving block decimation

1. Introduction

Frustrated spin systems have been a subject of interest because of their rich physics arising from competing interactions and quantum/thermal fluctuations.^{1,2} One-dimensional (1D) frustrated spin models provide one of the prototypical families to theoretically study unconventional orders with high accuracy. We here focus on the spin- $\frac{1}{2}$ XXZ chain with nearest-neighbor (NN) exchange coupling J_1 and next-nearest-neighbor (NNN) coupling J_2 . The Hamiltonian is given by

$$\mathcal{H} = \sum_{n=1,2} \sum_j J_n (S_j^x S_{j+n}^x + S_j^y S_{j+n}^y + \Delta S_j^z S_{j+n}^z). \quad (1)$$

Here Δ is the XXZ anisotropy, and we will consider the easy-plane region $0 \leq \Delta \leq 1$. In the case of antiferromagnetic (AF) $J_2 > 0$, NN and NNN couplings are geometrically frustrated irrespective of the sign of J_1 . This model has been studied in detail when J_1 and J_2 are both AF, and its ground-state and low-energy properties are now well understood.^{3,4,5,6,7,8} By contrast, relatively less is understood for the case of ferromagnetic (FM) J_1 and AF J_2 despite earlier studies.^{9,10,11,12} Recently, interest has been growing in this FM J_1 case because of its possible relevance

to several quasi-1D edge-sharing cuprates [LiCu₂O₂ (Ref. ¹³), LiCuVO₄ (Ref. ¹⁴), Rb₂Cu₂Mo₃O₁₂ (Ref. ¹⁵), PbCuSO₄(OH)₂ (Ref. ^{16,17}), etc.]. Some of these compounds exhibit multiferroic behavior in low-temperature spiral spin ordered phases, where the long-range order (LRO) of the vector spin chirality produces the electric polarization.^{18,19} Motivated by these developments, we have recently performed intensive studies on the ground-state phase diagram of the spin- $\frac{1}{2}$ J_1 - J_2 chain (1) with FM $J_1 < 0$ and AF $J_2 > 0$.^{20,21,22,23} In particular, among various phases which we have successfully characterized, the emergent LRO of the vector spin chirality for ferromagnetic J_1 with a weak easy-plane anisotropy would be relevant to quasi-1D multiferroic cuprates,²¹ when interchain couplings are taken into account.

The effect of external magnetic field is another interesting direction of research for the frustrated J_1 - J_2 spin chain systems. Recently, field-induced Tomonaga-Luttinger liquid (TLL) phases with spin multipolar quasi LRO have been theoretically investigated in the model (1),^{24,25} and it has been predicted that these multipolar phases show characteristic dynamical spin response which can be observed in NMR and neutron-scattering experiments.^{26,27,28} Throughout this paper, however, we restrict ourselves to the case at zero magnetic field. In the following sections, we review our recent results^{20,21,22,23} on the phase diagram and the characteristic features of the phases in the model (1). Including the parameter space of AF $J_1 > 0$, the phase diagram consists of at least six (and presumably more) kinds of distinct phases.

2. Competition between chiral and dimer orders

In this section, we consider the regime $-4 < J_1/J_2 < 4$ with $J_2 > 0$, where the classical ground state has an incommensurate spin spiral structure. This spiral state has a non-vanishing vector spin chirality $\kappa_j^z = \langle (\mathbf{S}_j \times \mathbf{S}_{j+1})^z \rangle \neq 0$. In the quantum case, a true spiral LRO with broken spin rotational symmetry is difficult to occur in 1+1 dimensions,²⁹ but a vector chiral LRO is allowed for $\Delta \neq 1$ since it only breaks a discrete \mathbb{Z}_2 symmetry.⁷ As explained below, this vector chiral order competes with several kinds of dimer orders driven by quantum fluctuations.

The ground-state phase diagram is presented in Fig. 1. The AF- J_1 side has been already established by several theoretical works. A strong enough AF NNN interaction J_2 causes a Kosteriz-Thouless (KT) transition from the TLL phase (connected to a single XXZ spin chain with the NN exchange coupling J_1) to a dimerized phase with spontaneously broken translational symmetry, in which the ground state is doubly degenerate.^{4,5} This dimer phase occupies a large part of the classical spiral regime $J_1/J_2 < 4$ of the AF- J_1 side. In fact, the ground state on the line $J_1/J_2 = 2$ and with $\Delta > -1/2$ (extension of the Majumder-Ghosh model³ at $\Delta = 1$) is given by a product state of singlet bonds, $|GS\rangle = \prod_{j=\text{even}} (|\uparrow\rangle_j |\downarrow\rangle_{j+1} - |\downarrow\rangle_j |\uparrow\rangle_{j+1})$ or $\prod_{j=\text{odd}} (|\uparrow\rangle_j |\downarrow\rangle_{j+1} - |\downarrow\rangle_j |\uparrow\rangle_{j+1})$, where $|\uparrow\rangle_j$ ($|\downarrow\rangle_j$) is the eigenstate of S_j^z with the eigenvalue $+1/2$ ($-1/2$). For later convenience, we introduce the xy

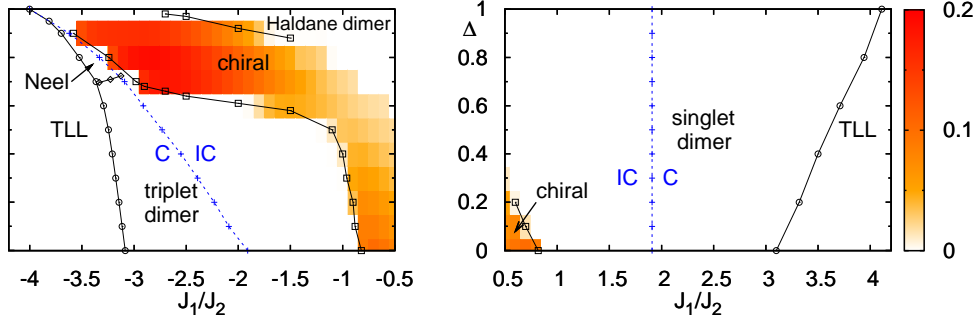


Fig. 1. Ground-state phase diagram of the J_1 - J_2 model (1) in the classically spiral regime $-4 \lesssim J_1/J_2 \lesssim 4$ with $J_2 > 0$. Strength of the vector chirality $\langle (\mathbf{S}_j \times \mathbf{S}_{j+1})^z \rangle$ calculated by iTEBD is also plotted with red color. The small Néel phase in the FM- J_1 side will be discussed in Sec. 3.

and z components of dimer order parameters

$$D_j^{xy} = \langle (S_{j-1}^x S_j^x + S_{j-1}^y S_j^y) - (S_j^x S_{j+1}^x + S_j^y S_{j+1}^y) \rangle, \quad (2)$$

$$D_j^z = \langle S_{j-1}^z S_j^z - S_j^z S_{j+1}^z \rangle. \quad (3)$$

For the above product state, we can easily show that (i) $\text{sign}(D_j^{xy}) = \text{sign}(D_j^z)$, and (ii) the energy density $\langle \mathbf{S}_j \cdot \mathbf{S}_{j+1} \rangle$ on the dimerized bond is negative. These properties persist in the whole region of the dimer phase in the AF- J_1 side. We call this phase the “singlet-dimer” phase. In this phase, there is a Lifshitz line across which the short-range spin correlation changes its character from commensurate to incommensurate (C and IC in Fig. 1).³⁰

In the weak J_1 region where $0 < J_1/J_2 \lesssim 0.8$, a vector-chiral phase appears^{7,8} in which the \mathbb{Z}_2 parity symmetry is spontaneously broken, and a nonvanishing and spatially uniform average of $\kappa_j^z = \langle (\mathbf{S}_j \times \mathbf{S}_{j+1})^z \rangle$ is found. In contrast to the dimer phase, the vector-chiral phase has a gapless excitation mode, and both the longitudinal and transverse spin correlation functions decay in a power-law fashion. In particular, the transverse spin correlator has an incommensurate oscillating factor.

Now, we turn to the FM- J_1 side, which has been investigated in our recent works.^{21,23} Phase boundaries are numerically determined by using infinite time evolving block decimation (iTEBD) method³¹ and numerical diagonalization. The phase diagram in Fig. 1 clearly shows that for $J_1 < 0$ the vector-chiral phase with $\kappa_j^z \neq 0$ appears for much broader parameter space than in the AF- J_1 case ($J_1 > 0$), and extends up to the vicinity of the SU(2) line $\Delta = 1$ for moderate values of $|J_1|/J_2$. This result naturally explains why quasi-1D J_1 - J_2 magnets with FM J_1 coupling often show a spiral spin order at low temperatures,^{13,14} while with AF J_1 coupling no quasi-1D magnet with a spiral order is found so far. Namely, a chiral ordered state appearing for realistically small easy-plane anisotropy $1 - \Delta \ll 1$ in the FM- J_1 side can be easily promoted to a 3D spiral ordered state by the addition of weak interchain couplings, while a gapped dimer state in the AF- J_1 side will be

robust against weak 3D couplings.

On the FM- J_1 side, there appear two distinct types of dimer phases between which the vector-chiral phase intervene in Fig. 1. The wider dimer phase appearing for strong easy-plane anisotropy $0 \leq \Delta \lesssim 0.6$ can be easily understood as follows.¹⁰ In the XY limit $\Delta = 0$, the spin chain with an AF NN coupling $J_1 = J > 0$ can be mapped to the same spin chain with the opposite sign of NN coupling ($J_1 = -J < 0$) through π rotation of spins around S^z axis on every second site. By this transformation a singlet dimer $|\uparrow\downarrow\rangle - |\downarrow\uparrow\rangle$ on a bond is changed into a triplet state $|\uparrow\downarrow\rangle + |\downarrow\uparrow\rangle$. Therefore, the ground state at $(J_1/J_2, \Delta) = (-2, 0)$ is a product state of triplet bonds, $|GS\rangle = \prod_{j=\text{even}}(|\uparrow\rangle_j|\downarrow\rangle_{j+1} + |\downarrow\rangle_j|\uparrow\rangle_{j+1})$ or $\prod_{j=\text{odd}}(|\uparrow\rangle_j|\downarrow\rangle_{j+1} + |\downarrow\rangle_j|\uparrow\rangle_{j+1})$. These states show $\text{sign}(D_j^{xy}) = -\text{sign}(D_j^z)$, and this property persists in the whole region of this dimer phase. We therefore call this phase the “triplet-dimer” phase. The singlet- and triplet-dimer phases can be distinguished by the signs of the dimer order parameters.

The nature of the other dimer phase around the SU(2) line $\Delta = 1$ has long been controversial. We have clarified some characteristic properties of this phase by applying unbiased iTEBD method. As shown in Fig. 2(a)(b) where dimer correlations are plotted for one of doubly degenerate ground states, the magnitude of dimer orders is quite tiny and $\text{sign}(D_j^{xy}) = \text{sign}(D_j^z)$ is realized. The latter property is the same as in the singlet-dimer phase. However, we have found that $\langle \mathbf{S}_j \cdot \mathbf{S}_{j+1} \rangle$ on a dimerized bond is positive, while it is negative in the singlet-dimer phase. This FM dimerization suggests that an effective spin-1 degree of freedom emerges on each of dimerized bonds. Therefore, we can expect a realization of a valence-bond-solid (VBS) state³² like in a spin-1 AF chain. In fact, the emergence of an effective spin-1 chain is very natural for FM J_1 coupling. To judge whether the dimer phase around $\Delta = 1$ can be well approximated by a VBS state, we calculate the string order parameter^{33,34}

$$O_{\text{str}}^\alpha(j-k) = - \left\langle (S_{2j}^\alpha + S_{2j+1}^\alpha) \exp \left[i\pi \sum_{l=j+1}^{k-1} (S_{2l}^\alpha + S_{2l+1}^\alpha) \right] (S_{2k}^\alpha + S_{2k+1}^\alpha) \right\rangle, \quad (4)$$

where we have assumed that bonds $(2l, 2l+1)$ are dimerized. Figure 2(c) clearly shows that the string parameter is long-range ordered. By contrast, the string order parameter defined on the non-dimerized bonds $(2l-1, 2l)$ is found to be short-ranged. We may expect that the dimer phase around $\Delta = 1$ should be adiabatically connected to a spin-1 AF chain if we introduce a strong FM bond alternation on J_1 bonds. (Note, however, that the dimerization is a spontaneous symmetry breaking in our model.) We thus call this phase the “Haldane-dimer” phase. Here, we leave the issue of whether this Haldane-dimer phase is adiabatically connected to the singlet-dimer phase or not for future studies.²³

Figure 2 suggests the presence of another type of dimer phase, in a narrow region of parameter space ($0.61 \lesssim \Delta \lesssim 0.65$ at $J_1/J_2 = -2$), which is characterized by coexisting dimer order D_j^{xy}, D_j^z and vector chirality κ_j^z . Let us call this phase

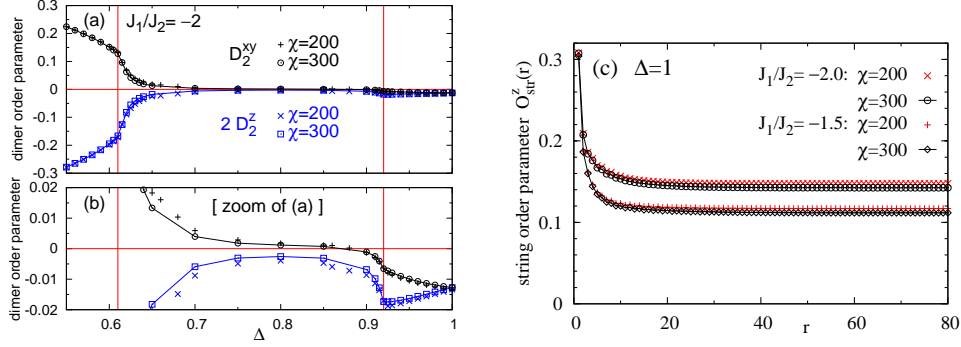


Fig. 2. (a) Δ dependence of dimer order parameters D_j^{xy} and D_j^z on $J_1/J_2 = -2$ line, calculated by iTEBD method with Schmidt rank $\chi = 200$ and 300. The chirality κ_j^z is finite between two vertical lines at $\Delta \simeq 0.61$ and $\Delta \simeq 0.92$. Panel (b) is a zoom of panel (a). (c) String order parameter (4) at points $(J_1/J_2, \Delta) = (-2, 1)$ and $(-1.5, 1)$ of the dimer phase, calculated by iTEBD method.

the “chiral-dimer” phase. We note that evaluated dimer order parameters in Fig. 2 cannot be used to determine the phase boundary between the chiral-dimer and vector-chiral phases. Further calculations are ongoing to verify the existence and to determine the range of this phase. More detailed discussions on the chiral, Haldane-dimer and chiral-dimer phases will be given in Ref. ²³.

3. Strong $|J_1|$ region: successive Néel-dimer transitions

In this section, we focus on the narrow region between the chiral and TLL phase around $-4 \lesssim J_1/J_2 \lesssim -3$. For such large negative J_1/J_2 , a single J_1 chain with $J_2 = 0$, which is exactly solvable, becomes a useful starting point. The low-energy effective Hamiltonian for the J_1 chain is a free boson (i.e., TLL) model with a nonlinear (vertex) term:

$$\mathcal{H}_{\text{eff}} = \frac{v}{2} \left[K (\partial_x \theta)^2 + \frac{1}{K} (\partial_x \phi)^2 \right] - \frac{v\lambda}{2\pi} \cos(\sqrt{16\pi}\phi), \quad (5)$$

where $x = ja$ (a is lattice spacing), $(\phi(x), \theta(x))$ is a pair of dual scalar fields, K is the TLL parameter, v is the spinon velocity, and λ is the coupling constant of the perturbative vertex term. For the J_1 chain with $0 \leq \Delta < 1$, the TLL parameter is given by $K = \pi/(2 \cos^{-1} \Delta)$. Since $K > 1$ in this case, the λ term (scaling dimension $4K$) is irrelevant in the renormalization-group sense, and a TLL phase is realized. Furthermore, the exact value of λ is known³⁵ and has an oscillating factor $-\sin(2\pi K)$ in the J_1 chain. Thus, λ changes its sign and becomes zero when $2K = n$, namely,

$$\Delta = \cos(\pi/n), \quad n = 3, 4, \dots \quad (6)$$

When small J_2 is introduced, the parameters K , v , and λ generally change, and finally the λ term becomes relevant and the TLL phase is destabilized towards

gapped phases.^{4,5} This boundary is determined in Ref. ¹², and is plotted by circular symbols interpolated by solid lines in Fig. 3(a). For the effective theory (5) it is known that, if the λ term is relevant, then positive λ induces a Néel order with finite $\langle S_j^z \rangle = -\langle S_{j+1}^z \rangle$, while negative λ induces a dimer order with finite $\langle \mathbf{S}_j \cdot \mathbf{S}_{j+1} - \mathbf{S}_{j+1} \cdot \mathbf{S}_{j+2} \rangle$. Thus a point of $\lambda = 0$ separates the dimer and Néel phases in the region with $4K < 2$. Using the level spectroscopy method of Ref. ⁵, we have determined the curves of $\lambda = 0$,²² which start from the points of Eq. (6) and are plotted as “+” symbols interpolated by broken lines. Remarkably, all the curves continue even outside the TLL phase. It means that successive dimer-Néel transitions occur as Δ is increased in the narrow region between TLL and chiral phases. In particular, the emergence of Néel order along S^z axis is nontrivial since it seems unfavored by both FM J_1 and AF J_2 couplings in the classical-spin picture.

The above argument has been based on the effective theory (5). Using unbiased iTEBD, we have also directly calculated the dimer and Néel order parameters along the Lifshitz line, where the order parameters are relatively large; see Fig. 3(b). We find that the transition points determined in Fig. 3 (a) and (b) are consistent.

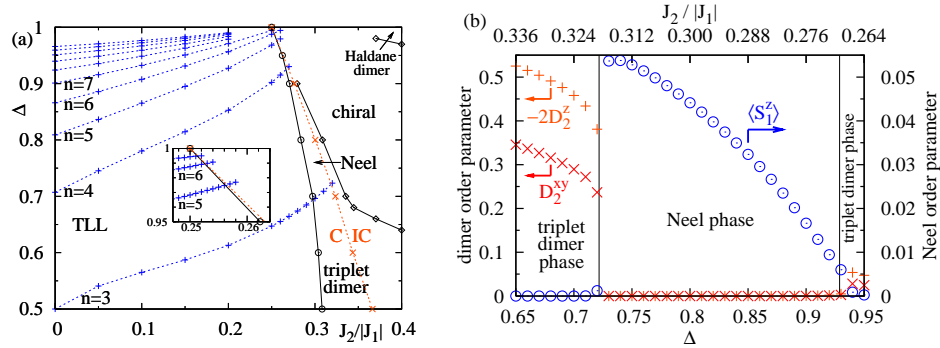


Fig. 3. (a) Ground-state phase diagram of the model (1) with FM $J_1 < 0$ for relatively small $J_2/|J_1|$. (b) Dimer and Néel order parameters, calculated by iTEBD method, along the Lifshitz line. The vertical lines indicate the phase boundaries determined by the level spectroscopy.

4. Summary

In this paper, we have discussed the ground-state properties of a spin- $\frac{1}{2}$ J_1 - J_2 chain (1) with easy-plane anisotropy, especially, for the FM- J_1 case. The ground-state phase diagram contains very rich physics: vector-chiral phase, four kinds of dimerized phases (singlet, triplet, Haldane and chiral dimers), Néel phases and TLL. Important findings in our recent studies on the FM- J_1 case include (i) remarkable stability of the vector-chiral phase even near $\Delta = 1$,²¹ (ii) a finite string order of the Haldane-dimer phase,²³ and (iii) successive Néel-dimer transitions.²² Furthermore, our numerical result suggests the possible coexistence of chirality and dimeriza-

tion in the narrow chiral-dimer phase.²³ More detailed properties of vector-chiral, Haldane-dimer, and chiral-dimer phases in FM- J_1 side will be discussed elsewhere.²³

Acknowledgments

This work was supported by Grants-in-Aid for Scientific Research from MEXT, Japan (Grants No. 21740295, and No. 22014016).

References

1. See, for a review, *Frustrated spin systems*, edited by H.T.Diep (World Scientific, Singapore, 2004).
2. See, for a review, L. Balents, *Nature* **464** (2010) 199.
3. C. K. Majumdar and D. K. Ghosh, *J. Math. Phys.* **10** 1399 (1969).
4. F.D.M. Haldane, *Phys. Rev.* **B25** (1982) 4925.
5. K. Nomura and K. Okamoto, *J. Phys.* **A27** (1994) 5773.
6. S.R. White, and I. Affleck, *Phys. Rev.* **B54** (1996) 9862.
7. A.A. Nersesyan, A.O. Gogolin, and F.H.L. Eßler, *Phys. Rev. Lett.* **81** (1998) 910.
8. T. Hikihara, M. Kaburagi, and H. Kawamura, *Phys. Rev.* **B63** (2001) 174430.
9. T. Tonegawa, I. Harada, and J. Igarashi, *Prog. Theor. Phys. Suppl.* **101** (1990) 513.
10. A. V. Chubukov, *Phys. Rev.* **B44** (1991) 4693.
11. C. Itoi and S. Qin, *Phys. Rev. B* **63** (2001) 224423.
12. R. D. Somma and A. A. Aligia, *Phys. Rev.* **B64** (2001) 024410.
13. T. Masuda, A. Zheludev, A. Bush, M. Markina, and V. Vasiliev, *Phys. Rev.* **B72** (2005) 014405.
14. M. Enderle, C. Mukherjee, B. Fåk, R. K. Kremer, J.-M. Broto, H. Rosner, S.-L. Drechsler, J. Richter, J. Malek, A. Prokofiev, W. Assmus, S. Pujol, J.-L. Raggazzoni, H. Rakoto, M. Rheinstädter, and H. M. Rønnow, *Europhys. Lett.* **70** (2005) 237.
15. M. Hase, H. Kuroe, K. Ozawa, O. Suzuki, H. Kitazawa, G. Kido, and T. Sekine, *Phys. Rev.* **B70** (2004) 104426.
16. G. Kamieniarz, M. Bieliński, G. Szukowski, R. Szymczak, S. Dyeyev, and J. -P. Renard, *Comp. Phys. Comm.* **147** (2002) 716.
17. M. Baran, A. Jedrzejczak, H. Szymczak, V. Maltsev, G. Kamieniarz, G. Szukowski, C. Loison, A. Ormeci, S.-L. Drechsler, and H. Rosner, *Phys. Stat. Sol. (c)* **3** (2006) 220.
18. H. Katsura, N. Nagaosa, and A. V. Balatsky, *Phys. Rev. Lett.* **95** (2005) 057205.
19. C. Jia, S. Onoda, N. Nagaosa, and J.H. Han, *Phys. Rev. B* **76** (2007) 144424.
20. S. Furukawa, M. Sato, Y. Saiga, and S. Onoda, *J. Phys. Soc. Jpn.* **77** (2008) 123712.
21. S. Furukawa, M. Sato, and S. Onoda, *Phys. Rev. Lett.* **105** (2010) 257205.
22. S. Furukawa, M. Sato, and A. Furusaki, *Phys. Rev.* **B81** (2010) 094430.
23. S. Furukawa, M. Sato, S. Onoda and A. Furusaki, *in preparation*.
24. T. Hikihara, L. Kecke, T. Momoi, and A. Furusaki, *Phys. Rev.* **B78** (2008) 144404.
25. J. Sudan, A. Luscher, and A.M. Läuchli, *Phys. Rev.* **B80** (2009) 140402(R).
26. M. Sato, T. Momoi and A. Furusaki, *Phys. Rev.* **B79** (2009) 060406(R).
27. M. Sato, T. Hikihara and T. Momoi, *Phys. Rev.* **B83** (2011) 064405.
28. M. Sato, T. Hikihara and T. Momoi, Proceedings of International Conference on Frustration in Condensed Matter (ICFCM) (2011); arXiv:1101.1375.
29. T. Momoi, *J. Stat. Phys.* **85** (1996) 193.
30. We have determined the C-IC boundary by looking at the peak position of the in-plane spin structure factor.

8 *Masahiro Sato*

31. G. Vidal, *Phys. Rev. Lett.* **98** (2007) 070201.
32. I. Affleck, T. Kennedy, E. H. Lieb and H. Tasaki, *Phys. Rev. Lett.* **59** (1987) 899;
Commun. Math. Phys. **115** (1988) 477.
33. M. den Nijs and K. Rommelse, *Phys. Rev.* **B40** (1989) 4709.
34. M. Kohmoto and H. Tasaki, *Phys. Rev.* **B46** (1992) 3486.
35. S. Lukyanov, *Nucl. Phys.* **B522** (1998) 533.